Supporting Information

Uyeda et al. 10.1073/pnas.1014503108

SI Text

Measures of Divergence and Time Intervals. We compiled datasets that measure evolutionary divergence in phenotypic traits from the following types of data: (*i*) contemporary field and historical studies, (*ii*) microgeographic divergence data where it can be inferred that there has been little to no gene flow between populations, (*iii*) fossil time series, and (*iv*) pairwise divergence between species on a phylogenetic tree. In each case, we standardized measures of divergence to compare data across traits, taxa, and time. We log-transformed all trait measurements so that divergence between any two samples is a unitless measure of the proportional change in a phenotypic trait in factors of *e*. Divergence between the means of two samples *a* and *b* is then measured simply as

$$d = (\overline{\ln z}_b - \overline{\ln z}_a)/k,$$

where $\overline{\ln z}_i$ is the mean of sample *i*. We corrected for dimensionality by dividing the difference in mean of the log-scaled trait values by *k*, where *k* is the dimensionality of the data (e.g., $k = 3$ for mass, $k = 2$ for area, and $k = 1$ for linear measurements). Time series data are commonly in the form

$$[(\overline{\ln z}_1, t_1), (\overline{\ln z}_2, t_2), \ldots, (\overline{\ln z}_{n-1}, t_{n-1}), (\overline{\ln z}_n, t_n)],$$

where the subscripts denote samples from earliest ($i = 1$) to the last ($i = n$), and t_i is the time elapsed between the *i*th and $(i + 1)$th sample. We measured *autonomous divergence* (1) as the difference between successive means in the series,

$$d = (\overline{\ln z}_{i+1} - \overline{\ln z}_i)/k.$$

The corresponding time interval is of length t_i. Some information is lost if only autonomous divergence is plotted, as longer trends in time series will not be represented. Consequently, we also calculated *nonautonomous divergence* (1) as the difference between sample means farther apart in the series, so that

$$d = \left(\overline{\ln z}_{i+j} - \overline{\ln z}_i\right)/k$$

is associated with a time interval of length

$$\sum_{l=i}^{i+j} t_l,$$

where $1 < j < n$. Nonautonomous divergence measures from the same series are not independent because they may be nested within one another or overlap, but they have the virtue of revealing trends in the mean over longer time intervals. Although this nonindependence can affect the significance of our model fits, it is unlikely to introduce a systematic bias in our parameter estimates or the visual appearance of the pattern given the large number of studies used. Consequently, whenever raw measurements were available, we included all pairwise comparisons between samples for a given time series, resulting in $n(n - 1)/2$ measures of nonautonomous divergence for a time series with *n* samples. We then averaged divergence values by binning the time series into $n - 1$ equally spaced intervals spanning the entire length of the series and averaging divergence values within each bin. Consequently, a maximum of $n - 1$ averaged nonautonomous data points were plotted for each time series and used in subsequent model fitting.

For the tree-based data, divergence was measured as

$$d = (\overline{\ln z}_b - \overline{\ln z}_a)/k,$$

where $\overline{\ln z}_a$ and $\overline{\ln z}_b$ are the log-transformed means for species *a* and *b*. Associated with *d* is the time interval, t_{ab}, calculated as the sum of the branch lengths from the most recent common ancestor to species *a* and *b*. We calculated *d* for all pairwise comparisons of species on the tree to give a visual sense of the range of divergence values. Because of the nonindependence of pairwise measures, we also averaged *d* and t_{ab} over comparisons spanning each node on the tree to reduce the influence of outlier species. In the case of contemporary longitudinal data (*allochronic*), we calculated *d*, where *a* and *b* represent two samples from a lineage separated by some known interval of time, t_{ab}. For contemporary cross-sectional data (*synchronic*), we measured *d* for two population samples and measured t_{ab} as twice the time since the most recent common ancestor of both populations *a* and *b*. We include only data in which we can infer limited to no gene flow between populations.

In many cases only trait means on an arithmetic scale were available. In those cases we approximated the mean of measurements on the log scale by taking the natural logarithm of the mean on the arithmetic scale. This approximation is good for symmetric distributions such as the normal distribution when the coefficient of variation is small, as is expected for most body size traits on the log scale. Furthermore, even if the distribution of log-scaled measurements is nonsymmetric and/or the SD is large, the distribution of divergence values will still closely approximate the true divergence value as long as the distributions of the traits in the two populations are similar.

An alternative measure of divergence is calculated as $h = d/\sigma_{ab}$ (corresponding to the haldane numerator), where σ_{ab} is the pooled within-population standard deviation (SD) of the log-transformed measurements from samples *a* and *b*, which can be approximated by the coefficient of variation. Gingerich (2) argued for standardization by σ_{ab} to remove the dimensionality of the data even for traits with unknown allometric scaling (e.g., shape traits, behavioral traits, and life-history traits), because σ_{ab} is itself proportional to the dimensionality of the data whereas standardization by *k* assumes a constant proportionality. However, standardization by σ_{ab} comes at the cost of standardization by an evolving and often poorly estimated quantity, and the exact dimensionality correction factor depends on the covariance structure of the lower-dimensional measurements (2, 3). Furthermore, for most morphometric variables proportionality changes are expected to be minimal for within-genus comparisons. Because linear divergence in size-related traits used in fossil time series and contemporary data reflect primarily a change in body size, the entire dataset approximates the evolution of a single trait (linear body mass), and the drawbacks of standardization by *k* are minimal. For simplicity, we present only data measured by divergence in *d* (Figs. 1 and 2) and present divergence in *h* for all traits in Fig. S1.

Datasets. We used the databases of Gingerich (3) and Hendry et al. (4), which included all of the data points used in Estes and Arnold (5), as well as additional studies (Table S2). We included the Gingerich (1) dataset, which measures standardized, autonomous divergence, h_a, in units of change per generation over timescales spanning a single generation to 10 million generations. Because we wanted to avoid biasing patterns by including traits observed over only one timescale and not the

other, we restricted our analysis to only traits related to body size of known dimensionality. In some instances we were able to convert some time series in this dataset to full sets of autonomous and nonautonomous divergence by using published raw data. However, because some of the time series in the Gingerich dataset were available only in terms of h, we had to approximate σ_{ab} to convert these values to d to obtain autonomous divergence values (for these datasets we did not estimate nonautonomous divergence). We estimated σ_{ab} for log-scaled linear measurements related to body size across mammalian taxa to determine the range of biologically realistic values. We collected measurements of variation from both fossil time series and contemporary populations to determine whether there are systematic differences between the estimates of variation in the two types of data. To supplement the fossil data, we used an online paleontology database (www.paleodb.org) and searched for mammalian taxa for which measures of variation were available. Estimated within-population SDs did not differ between population samples of extant species (mean SD ± 1 SD = 0.059 ± 0.03; 446 populations, 63 species) and fossil populations (mean SD ± 1 SD = 0.055 ± 0.03; 592 populations, 44 species), indicating that potential bias introduced by the different population sampling methods is minimal. We used these estimates to convert between the two standardizations for time series and comparative data for which measured SDs were not obtainable using a median value of 0.055. Although ideally measurements would be obtained from the actual populations for which the trait was measured, it has long been known that these values do not vary considerably for functional traits across mammalian taxa, even when evolutionary rates differ (6). Furthermore, the general pattern and identity of outlier taxa are consistent whether or not datasets are standardized by σ_{ab} or k (Fig. 1 and Fig. S1).

We supplemented these data with comparative, tree-based data on body-size divergence in mammals, birds, and squamates (Table S3). Measurements on body mass were taken from databases of body masses for extant birds and mammals to be matched to time-calibrated phylogenies (7, 8). Where multiple measurements were available for a single species, these were averaged to obtain a species-wide mean value. Divergence times for pairs of extant species were estimated as the sum the branch lengths separating taxa from their most recent common ancestor. For mammals, we used Bininda-Emonds et al.'s (9, 10) time-calibrated phylogeny to measure divergence time intervals. To obtain divergence between mammals in terms of generations rather than years, we obtained average generation times for 923 species from the PanTHERIA database and converted branch lengths by the mean of the generation time for the two species being compared (11). We also used a comparative dataset of molar size in 52 species of extant primates to compare with microevolutionary and paleontological studies of the same traits (mesio-distal length and trigonid breadth of the first molar) (12). When data on both male and female trait values are available, we assumed equal proportions of males and females to obtain an estimate of the species mean. For birds, we obtained intervals from phylogenies from McPeek's compilation of family- and genus-level time-calibrated phylogenies (13) and a supertree of the order Charadriiformes (14). For higher-level comparisons, we used the family-level phylogeny of Sibley and Ahlquist (15) scaled to a root age of 90 Myr. We then averaged body masses of all bird species within each family to use as the tip values and calculated the node-averaged divergence at each node in the phylogeny, which is equivalent to averaging all pairwise divergences for species means in monophyletic groupings. For squamate comparative data, we used Wiens et al.'s time-calibrated phylogeny and snout-to-vent length (SVL) measurements for a sample of 259 species (16).

We present divergence on the generation timescale (Fig. S2) to compare with divergence plotted on an absolute timescale (Fig. 1). Although qualitatively the pattern is consistent regardless of whether generations or years are used, the pattern of divergence is more consistent across taxa when measured on the raw timescale (Fig. 1), rather than generations (Fig. S2). There is a systematic bias for longer-lived organisms to diverge faster on the generation timescale than shorter-lived organisms (Fig. S2). However, there is no such obvious relationship between generation time and divergence patterns on the raw timescale. These results suggest that divergence over longer intervals scales with years rather than generations.

Stochastic Model Fitting. We fitted stochastic-process models to the combined datasets of node-averaged divergence values, the autonomous and averaged nonautonomous divergence values from fossil time-series data, and synchronic and allochronic microevolutionary divergence data. In addition, all models were fitted to subsets of the data including (*i*) microevolutionary and fossil data and (*ii*) phylogenetic data only. Our intent is to quantitatively elucidate features of the overall pattern by (*i*) evaluating the types of models that can explain the pattern and (*ii*) determining what parameter estimates are needed to explain the pattern. Accounting for the complex covariance structure of the data is beyond the scope of this paper and consequently we treated all data as independent. Violations of the assumption of independence are unlikely to systematically bias the conclusions we drew given the large and diverse nature of the dataset, although they will affect the magnitude of differences in AIC values for each model, and consequently these differences should be interpreted with caution. We further assume that all taxa have the same parameter values for each model. Although this assumption is clearly unrealistic, this preliminary modeling exercise is primarily aimed at identifying key general patterns that future models should account for and, as with Estes and Arnold (5), can be thought of as a screening procedure to synthesize data across a broad range of timescales and sources. The four models we tested are as follows.

1) Bounded-evolution (BE) model. We fitted a bounded-evolution model in which evolutionary changes are modeled as the differences between independent variables drawn from a normal distribution with zero mean and a constant variance, (σ_p^2), corresponding to a Gaussian white-noise process. This model is a special case of the models that follow and also corresponds to a special case of an Ornstein–Uhlenbeck process with an infinitely strong restraining force resulting in no serial autocorrelation between samples. Ornstein–Uhlenbeck processes are commonly used in comparative methods to model evolution toward an intermediate optimal state (17, 18). The probability distribution of divergence (x) contains only a single parameter, the variance of the stationary normal distribution (σ_p^2),

$$P(x) = \frac{1}{\sqrt{2\pi\sigma_p^2}} e^{-\frac{x^2}{2\sigma_p^2}}.$$

2) Brownian-motion (BM) model combined with white noise. This model describes the evolution of mean phenotypes by a random walk, but also has a time-independent component of variance, σ_p^2, as in the bounded evolution model. This time-independent variance could have contributions from multiple sources, including measurement error, phenotypic plasticity, genetic drift around a stationary optimum, or fluctuating selective pressures. The additional component of a random walk is modeled as Brownian motion with a stepwise infinitesimal variance parameter, σ_{bm}^2. The variance among replicate lineages of the Brownian motion process increases linearly with time according to the equation

$$\sigma_t^2 = \sigma_{\mathrm{bm}}^2 t,$$

where t is elapsed time. Under the influence of both constant white noise and random walk, the probability of a given level of

divergence after elapsed time t is a Gaussian probability density function with variance $\sigma_{\text{bm}}^2 t + \sigma_p^2$. The likelihood for this model then follows as the product of independent normal distributions, which yields the log-likelihood equation

$$\ln(L) = \sum_{n=1}^{n=N} \ln\left(\frac{e^{\frac{-x_n^2}{2(\sigma_p^2 + t\sigma_{\text{bm}}^2)}}}{\sqrt{2\pi(\sigma_p^2 + t\sigma_{\text{bm}}^2)}} \right).$$

3) Single-burst (SB) model with white noise. This model describes the process of evolution as a step function in which the mean of a lineage closely tracks an optimum that is displaced once and remains stationary thereafter. Under this model, most evolution occurs under a regime of stasis. We included this model because a displaced-optimum model was the best of several models examined by Estes and Arnold (5). In their model, the optimum was displaced in the first generation and remained stationary thereafter. We relaxed the constraint that the displacement occurs in the first generation and instead model the waiting time to displacement as an exponential distribution with parameter λ. Under this generalization of the model, displacements of the optimum are time dependent. Longer intervals are more likely to experience a displacement of the optimum, and therefore the variance in the magnitude of divergence values increases with time, as we now show. Let I be an indicator variable so that $I = 0$ when no displacement has occurred, and $I = 1$ when a displacement has occurred. Thus, for a single lineage the probability that a displacement has occurred in elapsed time t is given by the cumulative probability distribution of an exponential distribution:

$$P(I = 1) = 1 - e^{-\lambda t}.$$

Once the displacement occurs, the magnitude of the optimum's displacement, D, is drawn from a normal distribution with mean 0 and variance σ_D^2. Mean phenotypes are normally distributed about the expected optimum with variance σ_p^2. Consequently, the distribution of divergence values can be obtained by conditioning on I:

$$P(x) = P(x|I = 1) + P(x|I = 0)$$

$$P(x) = \frac{(1 - e^{-\lambda t})}{\sqrt{2\pi(\sigma_p^2 + \sigma_D^2)}} e^{\frac{-x^2}{2(\sigma_p^2 + \sigma_D^2)}} + \frac{(e^{-\lambda t})}{\sqrt{2\pi\sigma_p^2}} e^{\frac{-x^2}{2\sigma_p^2}}.$$

The likelihood for this model is calculated as the product of the marginal densities, resulting in the log-likelihood equation

$$\ln(L) = \sum_{n=1}^{n=N} \ln\left(\frac{(1 - e^{-\lambda t})}{\sqrt{2\pi(\sigma_p^2 + \sigma_D^2)}} e^{\frac{-x_n^2}{2(\sigma_p^2 + t\sigma_D^2)}} + \frac{(e^{-\lambda t})}{\sqrt{2\pi\sigma_p^2}} e^{\frac{-x_n^2}{2\sigma_p^2}} \right).$$

4) Multiple-bursts model with white noise. This model relaxes the assumption of a single displacement of the single-burst model and allows displacements to occur according to a Poisson process with rate parameter λ. According to this model, evolution consists predominantly of stasis interspersed with burst-like evolutionary events. If these burst events are sufficiently frequent over the interval examined, this model resembles the Brownian-motion model. If bursts are infrequent enough that the expected number of displacements is <1, then this model resembles the single-burst model. Under this model, the expected number of displacements, m, increases linearly with time and is equal to λt. The magnitudes of the displacements are drawn from $N(0, \sigma_D^2)$. As with the other models, we allowed for time-independent, bounded evolution that follows a normal distribution with variance, σ_p^2. Consequently, the probability distribution of divergence after m displacements is itself a normal distribution with mean 0 and variance, $\sigma_p^2 + m\sigma_D^2$. The probability distribution function can be obtained for this model by conditioning on the number of displacements, m, which follows a Poisson distribution:

$$P(x) = \sum_{m=0}^{m=\infty} P(x|m) = \sum_{m=0}^{m=\infty} \frac{e^{\left(\frac{-x^2}{2(\sigma_p^2 + m\sigma_D^2)}\right)}}{\sqrt{2\pi(\sigma_p^2 + m\sigma_D^2)}} p(m)$$
$$= \sum_{m=0}^{m=\infty} \frac{e^{\left(\frac{-x^2}{2(\sigma_p^2 + m\sigma_D^2)}\right)}}{\sqrt{2\pi(\sigma_p^2 + m\sigma_D^2)}} \frac{(\lambda t)^m e^{-\lambda t}}{m!}.$$

The likelihood function is then

$$\ln(L) = \sum_{n=1}^{n=N} \ln\left(\sum_{m=0}^{m=\infty} \frac{(\lambda t_n)^m e^{\left(\frac{-x_n^2}{2(\sigma_p^2 + m\sigma_D^2)} - \lambda t_n\right)}}{m!\sqrt{2\pi(\sigma_p^2 + m\sigma_D^2)}} \right).$$

Each model was fitted to the data by minimizing the negative log-likelihood function using the function *nlm* or *nlminb* in the R statistical computing environment (19). Because the number of data points provided by different studies varies widely and a single well-sampled study could substantially alter the overall model fit and parameter values, we bootstrapped over studies with 2,000 replicates for the best-fitting model (the multiple-burst model) to obtain a distribution of parameter values (Fig. S5).

Results and Interpretation of Model Fitting. For all datasets, the best-fitting model was the multiple-burst model. Note that this model is very similar to a Brownian-motion model for most of the time period examined. For the parameters examined, both the Brownian-motion and multiple-burst models predict nearly identical normal distributions of divergence measures up until ~1 Myr. Furthermore, the two processes have the same covariance structure (20). Consequently, the signal driving the improved support for the multiple-burst model in both the fossil and the comparative data is the overdispersed distribution of divergence between 1 Myr and 100 Myr. However, a Brownian-motion model could potentially produce such a distribution if modeled with a distribution of parameter values rather than a single parameter value. The single-burst model performs better than the Brownian-motion model for the same reason. However, this fitted single-burst model bears little resemblance to the best-fitting displaced-optimum model of Estes and Arnold (5). The difference arises because in their model, displacement of the optimum was constrained to occur in the first generation; thereafter the optimum remains stationary. In contrast, our model fit estimates that the mean time to displacement is over 25 Myr. In other words, the two models capture different phenomena in the data. The displaced-optimum model of Estes and Arnold (5) explains the central band of data that we model here as a consequence of a white-noise process and not the pattern of divergence observed on longer timescales that was fitted by our multiple-burst model (these longer timescales were not visible in the dataset examined by Estes and Arnold). In fact, when fitted to only the data with intervals <500,000 y, our displaced optimum model estimates the expected time to displacement as ~200 y and is the best fitting model among the four models we examined (Table S1). It is worth noting that Estes and Arnold

(5) reject a white-noise process for their data because the level of stochasticity in the optimum needed to obtain a reasonable fit would likely drive a population to extinction. Consequently, we use the white-noise process as a phenomenological model for the more complex processes that rapidly result in a static bounded distribution of divergence over microevolutionary timescales (<1 Myr). The Ornstein–Uhlenbeck process is an obvious modeling alternative that does not require high levels of stochasticity in the optimum (17, 18).

Measurement Error. We obtained reasonable estimates of the expected variance resulting from measurement error by using the median value for within-population SDs for linear body size traits and the sample sizes taken from the data. Sample sizes, however, were not available for most of the data. Consequently, we simulated sample sizes from a shifted geometric distribution with parameter 0.1 (giving a mean sample sample size of 10). We then drew sample means for two populations from a normal distribution with mean 0 and SD = 0.055. The 95% confidence interval was then obtained from the simulated distribution of measurement error. Our simulated distribution of sample sizes is a conservative estimate for microevolutionary studies, but a reasonable fit to the fossil data sample sizes. Although very few samples are represented by a single specimen, none of the divergence values we used were obtained from less than four total specimens. We obtained an estimate of measurement error of $\sigma_p = 0.04$, giving measurement variance of 0.0016. This value is nearly an order of magnitude less than the time-independent variance estimated from the data ($\hat{\sigma}_p^2 \approx 0.01$, Table 1). To obtain a variance of 0.01, assuming equal means, samples would have to consist of a single individual with within-population SDs of 0.07, a value higher than what is observed for most populations (median = 0.055). Because none of the data are represented by comparisons of such small samples, we reject the notion that measurement error alone is responsible for this significant time-independent component to variation in divergence.

Systematic bias resulting from differences in measurement error among data sources is unlikely to affect the observed pattern and alter our conclusions. As already noted, the variations in error from fossil and contemporary samples are often quite similar despite the diversity of taxa examined and the effects of time and geographic averaging, as has been found by previous authors (21–23). Consequently, differences in measurement error among sources will result primarily from systematic differences in sample sizes. For example, it is possible that measurement error could result in the appearance of stasis if there is an inverse relationship between the amount of measurement error and the length of the interval, where measurement error decreases with increasing intervals. Such an inverse relationship is unlikely because contemporary field studies have the highest sample sizes in the dataset and are least affected by measurement error. Similarly, the expansion of variance that occurs after 1 Myr could result if phylogenetic comparative data were significantly more variable than paleontological data. However, this difference is likewise highly unlikely because the magnitude of the effect is so large, and estimates of divergence are based on contemporary measurements that have reasonable sample sizes [median $n = 12$ and $n = 11$ per species for reported values in Dunning (8) and Swindler (12), respectively]. Furthermore, variance in divergence in phylogenetic data is less that in than paleontological data collected over the same time intervals (Fig. S3).

Linear Regressions of Absolute Divergence on Time. To determine whether the pattern between datasets was better explained by a subdividing by dataset or by designating a specific breakpoint, we compared separate linear regressions fitted to each dataset with a segmented regression with a single breakpoint. We log-transformed the absolute value of the response variable, $|d|$ and added a small fixed deviate (0.001) to obtain an approximately normal distribution of divergence values. All of the data points included in the stochastic modeling analysis were also analyzed here. The transformed data are expected to have a linear relationship with log interval under a Brownian-motion model. We then compared three models: (*i*) a single linear regression fit to the combined dataset (two parameters), (*ii*) a model in which each dataset was fitted independently (resulting in three independent linear regressions and six parameters), and (*iii*) a segmented regression model with a single breakpoint (four parameters). The segmented regression model allowed for a change in slope, but constrained the lines to connect, resulting in four parameters (two slope parameters for before and after the breakpoint, the initial intercept, and the breakpoint itself). We determined the optimal breakpoint by iteratively fitting the segmented regression model to the data by increasing the breakpoint value from 0 to 8.5 $\log_{10}$ y, with a step value of 0.01. The lowest AIC value is obtained at a breakpoint of ~66,000 y (Fig. 4). Models were compared using AIC calculated from the residual sum of squares. Care should be taken in interpreting the AIC scores, as violations of independence in the data will exaggerate the differences between models. Nonetheless, we found that the hybrid nature of the dataset contributes less to the change in pattern of divergence than the change in timescale.

1. Gingerich PD (2001) Rates of evolution on the time scale of the evolutionary process. *Genetica* 112–113:127–144.
2. Gingerich PD (1993) Quantification and comparison of evolutionary rates. *Am J Sci* 293:453–478.
3. Lande R (1977) On comparing coefficients of variation. *Syst Zool* 26:214–217.
4. Hendry AP, Farrugia TJ, Kinnison MT (2008) Human influences on rates of phenotypic change in wild animal populations. *Mol Ecol* 17:20–29.
5. Estes S, Arnold SJ (2007) Resolving the paradox of stasis: Models with stabilizing selection explain evolutionary divergence on all timescales. *Am Nat* 169:227–244.
6. Simpson GG (1944) *Tempo and Mode in Evolution* (Columbia Univ Press, New York).
7. Smith F, et al. (2003) Body mass of late Quaternary mammals. *Ecology* 84:3403.
8. Dunning JB (1993) *CRC Handbook of Avian Body Masses* (CRC Press, Boca Raton, FL), 2nd Ed.
9. Bininda-Emonds ORP, et al. (2007) The delayed rise of present-day mammals. *Nature* 446:507–512.
10. Bininda-Emonds ORP, et al. (2008) The delayed rise of present-day mammals. *Nature* 456:274.
11. Jone KE, et al. (2009) PanTHERIA: A species-level database of life history, ecology, and geography of extant and recently extinct mammals. *Ecology* 90:2648.
12. Swindler DR (2002) *Primate Dentition* (Cambridge Univ Press, Cambridge, UK).
13. McPeek MA (2008) The macrocecological dynamics of clade diversification and community assembly. *Am Nat* 172:E270–E284.
14. Thomas G, Wills M, Szekely T (2004) A supertree approach to shorebird phylogeny. *BMC Evol Biol* 4:28.
15. Sibley CG, Ahlquist JE (1990) *Phylogeny and Classification of Birds: A Study in Molecular Evolution* (Yale Univ Press, New Haven, CT).
16. Wiens JJ, Brandley MC, Reeder TW (2006) Why does a trait evolve multiple times within a clade? Repeated evolution of snakelike body form in squamate reptiles. *Evolution* 60:123–141.
17. Hansen TF (1997) Stabilizing selection and the comparative analysis of adaptation. *Evolution* 51:1341–1351.
18. Butler MA, King AA (2004) Phylogenetic comparative analysis: A modeling approach for adaptive evolution. *Am Nat* 164:683–695.
19. R Development Core Team (2009) *R: A Language and Environment for Statistical Computing* (R Foundation for Statistical Computing, Vienna). Available at http://www.R-project.org. Accessed September, 2009.
20. Hansen TF, Martins EP (1996) Translating between microevolutionary process and macroevolutionary patterns: The correlation structure of interspecific data. *Evolution* 50:1404–1417.
21. Bell MA, Sadagursky MS, Baumgartner JV (1987) Utility of lacustrine deposits for the study of variation within fossil samples. *Palaios* 2:455–466.
22. Bush AM, et al. (2002) Time-averaging, evolution and morphologic variation. *Paleobiology* 28:9–25.
23. Hunt G (2004) Phenotypic variation in fossil samples: Modeling the consequences of time-averaging. *Paleobiology* 30:426–443.

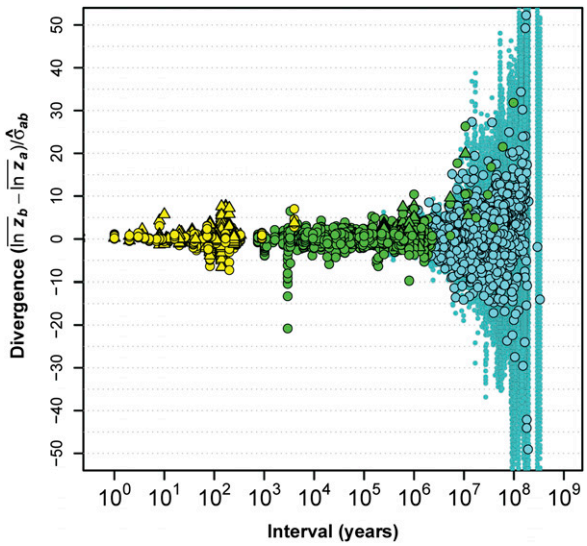

Fig. S1. Divergence between populations in all types of traits standardized by their pooled within-population SD for log-scaled trait values (corresponding to the Haldane numerator). Size traits are indicated by circles, and all others are indicated by triangles (including shape, behavior, life history traits, coloration, etc.). Datasets are colored according to data type: microevolutionary, yellow; fossil, green; and comparative, blue. All measurements of divergence for comparative data are standardized by a median value of the SD of log-scaled linear body size traits of $\sigma_{ab} = 0.055$.

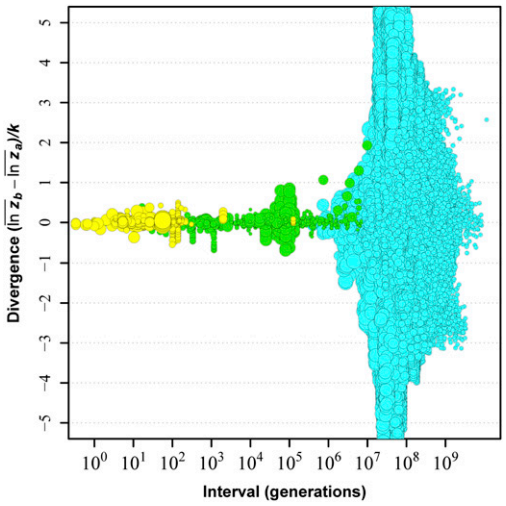

Fig. S2. Body-size divergence as a function of generations rather than years. Colors are the same as in Fig. S1. The size of the points is proportional to the log of generation time. Generation times for comparative data are estimated as the mean generation time of the two species being compared (available for mammals only, pairwise only). Note that in all datasets, there is a tendency for more rapid divergence in organisms with longer generation times and delayed divergence for organisms with shorter generation times. This apparently systematic difference in divergence patterns suggests that divergence does not scale with generations, but rather scales with years (compare with Fig. 1).

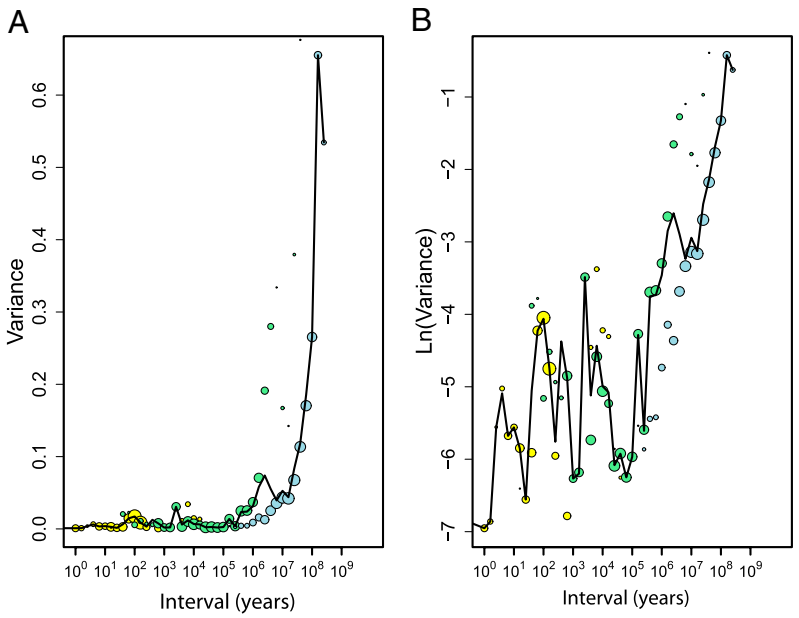

Fig. S3. (*A*) Among-lineage variance through time plot for each dataset individually (microevolutionary, yellow; fossil, green; phylogenetic, blue) and all three categories combined (black line). Variance is calculated from the data binned at every 0.1 unit on the $\log_{10}$ interval scale. The size of the data points is proportional to the natural log of the number of data points included in that bin. Note that the fossil data appear to accumulate variance faster than the phylogenetic data. (*B*) Same plot as before, but variance is ln-transformed. Note the nearly linear accumulation of variance after $\sim 10^5$–10^6 y.

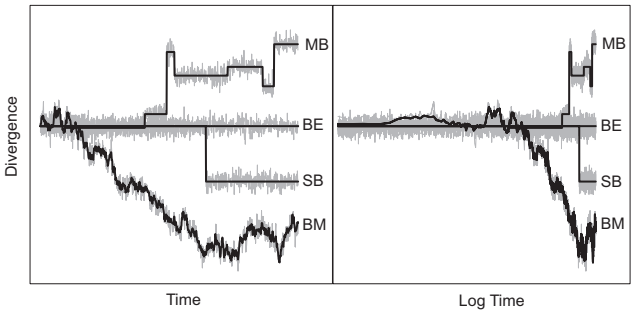

Fig. S4. Simulated realizations of each model that we fitted to the data displayed on both the raw timescale (*Left*) and the log-transformed timescale (*Right*). The models are a bounded-evolution model (BE), a Brownian-motion model with white noise (BM), single-burst model (SB), and a multiple-burst model (MB). Shaded lines are the bounded-evolution process (BE) around each underlying process model, which is the solid line. Parameter values chosen for these simulations are arbitrary, but a common white-noise parameter, σ_p^2, is used in each model. Note that when time is on the log scale, divergence is primarily described by the white-noise parameter over much of the timespan, whereas at longer timescales it is primarily described by the underlying stochastic process model.

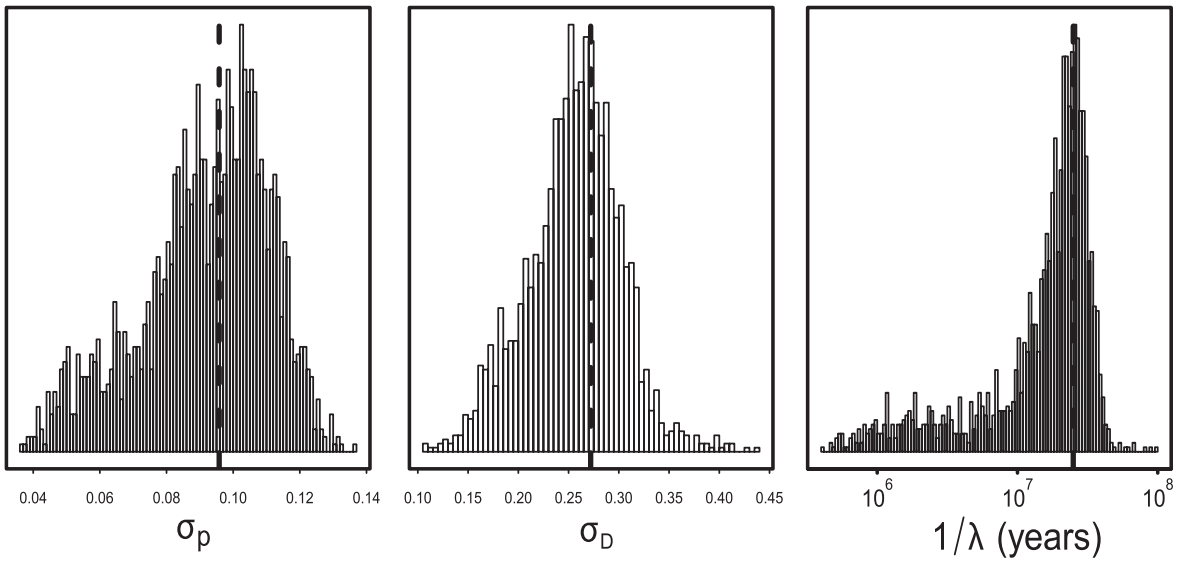

Fig. S5. Parameter distributions from the Poisson process model (MB) obtained by bootstrapping over studies (2,000 replicates). Dashed lines indicate the position of the estimated parameter from the full dataset (Table 1). Strong positive correlations exist between all parameter values, with correlations ranging from 0.68 to 0.87.

Table S1. Parameter estimates and AIC scores for three model fits to the data

Dataset	Model	Parameter estimates			AIC
Microevolution and fossil	BE	$\hat{\sigma}_p = 0.1417$			−5740.28
	BM	$\hat{\sigma}_p = 0.0974$	$\hat{\sigma}_{bm} = 1.60\times10^{-4}$		−8298.53
	SB	$\hat{\sigma}_p = 0.0885$	$\hat{\sigma}_D = 0.396$	$1/\hat{\lambda} = 10^{6.2990}$	−8687.00
	MB	$\hat{\boldsymbol{\sigma}}_{\boldsymbol{p}} = \mathbf{0.0874}$	$\hat{\boldsymbol{\sigma}}_{\boldsymbol{D}} = \mathbf{0.249}$	$\mathbf{1}/\hat{\lambda} = \mathbf{10}^{\mathbf{6.1642}}$	**−8793.06**
Phylogenetic only	BE	$\hat{\sigma}_p = 0.2986$			1106.31
	BM	$\hat{\sigma}_p = 0.1000$	$\hat{\sigma}_{bm} = 4.61\times10^{-5}$		0.66
	SB	$\hat{\sigma}_p = 0.1182$	$\hat{\sigma}_D = 0.4451$	$1/\hat{\lambda} = 10^{7.7344}$	−171.30
	MB	$\hat{\boldsymbol{\sigma}}_{\boldsymbol{p}} = \mathbf{0.0857}$	$\hat{\boldsymbol{\sigma}}_{\boldsymbol{D}} = \mathbf{0.2166}$	$\mathbf{1}/\hat{\lambda} = \mathbf{10}^{\mathbf{7.3375}}$	**−363.26**
All data <500,000 y	BE	$\hat{\sigma}_p = 0.0976$			−8493.74
	BM	$\hat{\sigma}_p = 0.0976$	$\hat{\sigma}_{bm} = 1.94\times10^{-7}$		−8491.74
	SB	$\hat{\boldsymbol{\sigma}}_{\boldsymbol{p}} = \mathbf{0.0260}$	$\hat{\boldsymbol{\sigma}}_{\boldsymbol{D}} = \mathbf{0.106}$	$\mathbf{1}/\hat{\lambda} = \mathbf{10}^{\mathbf{2.276}}$	**−8960.72**
	MB	$\hat{\sigma}_p = 0.0872$	$\hat{\sigma}_D = 0.327$	$\mathbf{1}/\hat{\lambda} = 10^{6.337}$	−8758.38
All data >500,000 y	BE	$\hat{\sigma}_p = 0.2997$			1417.48
	BM	$\hat{\sigma}_p = 0.1946$	$\hat{\sigma}_{bm} = 3.99\times10^{-5}$		599.30
	SB	$\hat{\sigma}_p = 0.1558$	$\hat{\sigma}_D = 0.508$	$\mathbf{1}/\hat{\lambda} = 10^{7.8724}$	105.76
	MB	$\hat{\boldsymbol{\sigma}}_{\boldsymbol{p}} = \mathbf{0.1480}$	$\hat{\boldsymbol{\sigma}}_{\boldsymbol{D}} = \mathbf{0.361}$	$\mathbf{1}/\hat{\lambda} = \mathbf{10}^{\mathbf{7.7482}}$	**45.82**

Models tested include a bounded-evolution model (BE), a Brownian-motion model (BM), a single-burst model (SB), and a multiple-burst model (MB). In all models, SDs are in units of the natural log size difference. The inverse of the rate parameters ($1/\lambda$) for the exponential distribution and Poisson distribution in the single-burst and multiple-burst models, respectively, can be interpreted as the average number of years until a displacement. Details of each model can be found in *SI Text*. Best-fitting model for each dataset is indicated in bold.

Table S2. Data sources for microevolutionary and paleontological data used in this study

Taxa	Source	Species	Original database	Type of study	No. of divergence points, *d* (*h* only)	No. of measured traits in study, *d* (*h* only)	No. of populations, *d* (*h* only)
Aves	Baker, 1980	*Passer domesticus*	(1)	Field-syn	312	2	13
Aves	Baker, 1990	*Fringilla coelebs*	(1)	Field-syn	336	12	8
Rodentia	Berry, 1964	*Mus musculus*	(1)	Field-syn	2 (1)	2 (1)	2
Salmonidae	Bielak and Powers, 1986	*Salmo salar*	(1)	Field-allo	2	1	4
Salmonidae	Bigler et al., 1996	*Oncorhynchus gorbuscha*	(1)	Field-allo	55 (11)	2 (1)	64 (22)
Insecta	Carroll et al., 1997	*Jadera hematoloma*	(1)	Field-syn	50 (16)	3 (1)	9
Insecta	Carroll et al., 1998	*J. hematoloma*	(1)	Field-syn	20 (16)	2 (2)	9
Aves	Clegg et al., 2002	*Zosterops lateralis*	(1)	Field-syn	40	10	5
Salmonidae	Cox and Hinch, 1997	*Oncorhynchus nerka*	(1)	Field-allo	20	1	20
Poecilidae	Endler, 1980	*Poecilia reticulata*	(1)	Field-syn	2 (2)	2 (2)	1
Aves	Grant and Grant, 1995	*Geospiza fortis*	(1)	Field-allo	12	6	4
Salmonidae	Haugen and Vøllestad, 2001	*Thymallus thymallus*	(1)	Field-syn	36 (18)	12 (6)	3
Salmonidae	Haugen, 2000	*T. thymallus*	(1)	Field-syn	25 (23)	4 (3)	15 (5)
Salmonidae	Hendry and Quinn, 1997	*Oncorhynchus nerka*	(1)	Field-syn	16	2	3
Salmonidae	Hendry et al., 1998	*O. nerka*	(1)	Field-syn	0 (2)	0 (2)	0 (2)
Insecta	Hill et al., 1999	*Pararge aegeria*	(1)	Field-syn	4	1	4
Insecta	Huey et al., 2000	*Drosophila subobscura*	(1)	Field-syn	2	1	2
Aves	Johnston and Selander, 1964	*Passer domesticus*	(1)	Field-syn	126	3	17
Salmonidae	Kinnison, 1998	*Oncorhynchus tshawytscha*	(1)	Field-syn	6 (6)	3 (6)	7
Gasterosteodae	Klepaker, 1993	*Gasterosteus aculeatus*	(1)	Field-syn	44	1 (21)	1 (2)
Aves	Larsson et al., 1998	*Branta leucopsis*	(1)	Field-allo	8	2	4
Poecilidae	Magurran et al., 1992	*Poecilia reticulata*	(1)	Field-syn	0 (2)	0 (1)	0 (2)
Poecilidae	Magurran et al., 1995	*P. reticulata*	(1)	Field-syn	0 (2)	0 (1)	0 (2)
Mollusca	McMahon, 1976	*Physa virgata*	(1)	Field-syn	0 (3)	0 (3)	0 (2)
Rodentia	Pergams and Ashley, 1999	*Peromyscus maniculatus*	(1)	Field-allo	48	16	6
Poecilidae	Reznick and Bryga, 1987	*P. reticulata*	(1)	Field-syn	3 (2)	2 (2)	2
Poecilidae	Reznick et al., 1990	*P. reticulata*	(1)	Field-syn	8 (11)	6 (6)	4
Poecilidae	Reznick et al., 1997	*P. reticulata*	(1)	Field-syn	6 (6)	1 (1)	5
Aves	Smith et al., 1995	*Vestiaria coccinea*	(1)	Field-allo	5	5	2
Aves	St.Louis and Barlow, 1991	*Passer domesticus*	(1)	Field-syn	32	16	2
Poecilidae	Stearns, 1983b	*Gambusia affinis*	(1)	Field-syn	45 (30)	2 (1)	1
Poecilidae	Stearns, 1983a	*G. affinis*	(1)	Field-syn	808 (277)	3 (1)	36
Poecilidae	Stockwell and Leberg, 2000	*G. affinis*	(1)	Field-syn	12 (6)	2 (1)	4
Mollusca	Trussell and Smith, 2000	*Littorina obtusata*	(1)	Field-syn	10	2	8
Mollusca	Vermeij, 1982	*Nucella lapillus*	(1)	Field-allo	8	2	8
Lagomorpha	Williams and Moore, 1989a	*Oryctolagus cuniculus*	(1)	Field-syn	0 (24)	0 (4)	0 (3)
Lagomorpha	Williams and Moore, 1989b	*O. cuniculus*	(1)	Field-syn	27	9	3
Aves	Zink, 1983	*Passerella iliaca*	(1)	Field-allo	31	31	2
Gasterosteodae	Bell et al., 2004	*Gasterosteus aculeatus*	(1)	Field-allo	0 (4)	0 (1)	0 (5)
Diptera	Bradshaw and Holzapfel, 2001	*Wyeomyia smithii*	(1)	Field-allo	0 (2)	0 (1)	0 (4)
Squamata	Campbell and Echternacht, 2003	*Anolis sagrei*	(1)	Field-allo	10	2	6
Insecta	Carroll et al., 2001	*Jadera hematoloma*	(1)	Field-syn	3 (2)	2 (1)	2
Insecta	Carroll et al., 2005	*J. hematoloma*	(1)	Field-syn	14	4	2
Artiodactyla	Coltman et al., 2003	*Ovis canadensis*	(1)	Field-allo	2	2	2
Aves	Conant, 1988	*Telespyza cantans*	(1)	Field-syn	18	3	3
Aves	Cooch et al., 1991	*Anser caerulescens*	(1)	Field-allo	4	3	8

Table S2. Cont.

Taxa	Source	Species	Original database	Type of study	No. of divergence points, *d* (*h* only)	No. of measured traits in study, *d* (*h* only)	No. of populations, *d* (*h* only)
Diptera	Gilchrist et al., 2001	*Drosophila subobscura*	(1)	Field-allo	48	3	16
Diptera	Gilchrist et al., 2004	*D. subobscura*	(1)	Field-syn	6	3	2
Salmonidae	Handford et al., 1977	*Coregonus clupeaformis*	(1)	Field-allo	2 (1)	2 (1)	2
Centrarchidae	Holland et al., 1974	*Lepomis macrochirus*	(1)	Field-syn	0 (9)	0 (1)	0 (9)
Salmonidae	Kinnison et al., 2003	*Oncorhynchus tsawytscha*	(1)	Field-syn	5	4	2
Oligochaeta	Levinton et al., 2003	*Limnodrilus hoffmeisteri*	(1)	Field-allo	0 (1)	0 (1)	0 (2)
Poecilidae	Meffe et al., 1995	*Gambusia holbrooki*	(1)	Field-syn	0 (2)	0 (2)	0 (2)
Artiodactyla	Milner et al., 1999	*Ovis aries*	(1)	Field-allo	12	3	6
Aves	Moller and Szep, 2005	*Hirundo rustica*	(1)	Field-allo	2	1	2
Rodentia	Pergams and Ashley, 2001	*Mus musculus*	(1)	Field-syn	29	13	8
Anura	Phillips and Shine, 2005	*Bufo marinus*	(1)	Field-allo	2	1 (1)	1 (1)
Aves	Postma and van Noordwijk, 2005	*Parus major*	(1)	Field-syn	0 (2)	0 (2)	0 (2)
Aves	Rasner et al., 2004	*Junco hyemalis*	(1)	Field-syn	4	2	2
Cichlidae	Streelman et al., 2004	*Cynotilapia afra*	(1)	Field-syn	0 (15)	0 (1)	0 (6)
Crustacea	Tessier et al., 1992	*Daphnia galeata mendotae*	(1)	Field-allo	4 (3)	4 (3)	2
Aves	Clegg et al., 2008,	*Zosterops lateralis*	(1)	Field-syn	7	7	2
Artiodactyla	Smith et al., 2003	Introduced Australian artiodactyls	This paper	Field-syn	13	1	4
Carnivora	Simberloff, 2000	*Herpestes javanicus*	This paper	Field-syn	98	2	8
Xenarthra	Anderson and Handley, 2002	*Bradypus*	This paper	Field-syn	7	1	8
Rodentia	Smith et al., 1998	*Neotoma*	This paper	Field-allo	8	1	1
Primates	Cuozzo and Sauther, 2006	*Lemur catta*	This paper	Field-allo	27	9	1
Primates	DeGusta et al., 2003	*Alouatta palliata*	This paper	Field-allo	6	1	4
Rodentia	Milien, 2004	*Apodemus argentatus*	This paper	Field-syn	5	1	6
Primates	O'Rourke and Crawford, 2004	*Homo sapiens*	This paper	Field-syn	52	26	2
Squamata	Pregill, 1986	*Anolis bimaculatis*	This paper	Field-syn	6	6	2
Squamata	Meiri, 2007*	Island-mainland lizards	This paper	Field-syn	25	1	29
Squamata	Meik et al., 2010	*Crotalus mitchelli*	This paper	Field-syn	12	1	14
Insecta	Santos et al., 1992	*Drosophila buzzatii*	This paper	Field-allo	8	2	4
Rodentia	Bouteiller-Reuter and Perrin, 2005	*Crocidura russula*	This paper	Field-allo	6	2	3
Amphibia	Wagner and Sullivan, 1995	*Bufo valliceps*	This paper	Field-allo	3	1	3
Squamata	Olsson and Madsen, 2001	*Lacerta agilis*	This paper	Field-allo	1	1	2
Squamata	Herrel et al., 2008	*Podarcis sicula*	This paper	Field-syn	20	10	2
Condricthyes	DiBattista et al., 2007	*Negaprion brevirostris*	This paper	Field-allo	0 (22)	4	6
Rodentia	Hester, n.d.	*Peromyscus*	(2)	Field-allo	9	1	10
Perissodactyla	Gingerich, 1991	*Hyracotherium grangeri*	(2)	Fossil ts	42	2	22
Perissodactyla	Forsten, 1990	*Equus germanicus*	(2)	Fossil ts	204	34	7
Rodentia	Lich, 1990	*Cosomys primus*	(2)	Fossil ts	27	3	10
Proprimates	Gingerich and Gunnell, 1995	*Phenacolemur praecox*	(2)	Fossil ts	40	2	21
Primates	Gingerich and Gunnell, 1995	*Tetonius steini–T. homunculus*	(2)	Fossil ts	26	2	14
Primates	Gingerich and Gunnell, 1995	*Teilhardina amer.–T. tenuicula*	(2)	Fossil ts	18	2	10
Primates	Clyde and Gingerich, 1994	*Cantius torresi–C. trigonodus*	(2)	Fossil ts	78	2	40

Table S2. Cont.

Taxa	Source	Species	Original database	Type of study	No. of divergence points, *d* (*h* only)	No. of measured traits in study, *d* (*h* only)	No. of populations, *d* (*h* only)
Creodonta	Gingerich and Gunnell, 1995	*Arfia junnei–A. opisthotoma*	(2)	Fossil ts	24	2	13
Condylarthra	Gingerich, 1994	*Haplomylus speir.–H. scott*	(2)	Fossil ts	70	2	36
Condylarthra	Gingerich, 1994	*Hyopsodus loomisi*	(2)	Fossil ts	52	2	27
Condylarthra	Gingerich, 1994	*Hyopsodus latidens*	(2)	Fossil ts	32	2	17
Condylarthra	Gingerich and Gunnell, 1995	*Hyopsodus lo:la*	(2)	Fossil ts	2	2	2
Condylarthra	Gingerich and Gunnell, 1995	*Thryptacodon antiquus*	(2)	Fossil ts	28	2	15
Condylarthra	Gingerich and Gunnell, 1995	*Ectocion osbornianus*	(2)	Fossil ts	46	2	24
Condylarthra	Gingerich and Gunnell, 1995	*Phenacodus vortmani*	(2)	Fossil ts	42	2	22
Condylarthra	Gingerich and Gunnell, 1995	*Phenacodus n. sp.*	(2)	Fossil ts	52	2	27
Condylarthra	Gingerich and Gunnell, 1995	*Phenacodus intermedius*	(2)	Fossil ts	22	2	12
Tillodontia	Gingerich and Gunnell, 1995	*Azygonyx xenicus–A. grangeri*	(2)	Fossil ts	22	2	12
Tillodontia	Gingerich and Gunnell, 1995	*Esthonyx spat.–E. bisulcatus*	(2)	Fossil ts	36	2	19
Artiodactyla	Gingerich and Gunnell, 1995	*Diacodexis metsiacus*	(2)	Fossil ts	58	2	30
Perissodactyla	Gingerich and Gunnell, 1995	*Cardiolophus radinskyi*	(2)	Fossil ts	24	2	13
Perissodactyla	Gingerich and Gunnell, 1995	*Homogalax protapirinus*	(2)	Fossil ts	20	2	11
Rodentia	Jacobs and Lindsay, n.d.	*Potwarmus prim.–Mus auctor*	(2)	Fossil ts	54	2	28
Rodentia	Flynn, 1986	*Kanisamys indicus–K. sival.*	(2)	Fossil ts	38	2	20
Rodentia	Jacobs, n.d.	*Karnimata sp.–K. huxleyi*	(2)	Fossil ts	18	2	10
Rodentia	Jacobs, n.d.	*Karnimata sp.–Parapelomys rob.*	(2)	Fossil ts	12	2	7
Artiodactyla	Morgan, n.d.	*Bramatherium megacephalus*	(2)	Fossil ts	12	1	13
Artiodactyla	Morgan, n.d.	*Giraffokeryx punjabiensis*	(2)	Fossil ts	15	1	16
Condylarthra	Gingerich, 1994	*Apheliscus chydaeus*	(2)	Fossil ts	26	2	14
Proprimates	Gingerich, 1996	*Pronoth. jepi–Ples. churchilli*	(2)	Fossil ts	6	2	4
Proprimates	Gingerich, 1996	*Ples. churchilli–Ples. dubius*	(2)	Fossil ts	18	2	10
Proprimates	Gingerich, 1996	*Ples. churchilli–Ples. cookei*	(2)	Fossil ts	24	2	13
Proprimates	Bloch and Gingerich, 1998	*Carpolestes spp.*	(2)	Fossil ts	24	2	13
Proprimates	Bloch and Gingerich, 1998	*Carpolestes spp.*	(2)	Fossil ts	26	2	14
Proprimates	Bloch and Gingerich, 1998	*Carpolestes spp.*	(2)	Fossil ts	24	2	13
Perissodactyla	Gingerich, 1991	*Hyracotherium aemulor*	(2)	Fossil ts	22	2	12
Perissodactyla	Gingerich, 1991	*Hyracotherium pernix*	(2)	Fossil ts	6	2	4
Perissodactyla	Gingerich, 1991	*Hyracotherium sa:gr:ae:pe*	(2)	Fossil ts	6	6	2
Proboscidea	King and Saunders, 1984	*Mammut americanum*	(2)	Fossil ts	8	4	3

Table S2. Cont.

Taxa	Source	Species	Original database	Type of study	No. of divergence points, *d* (*h* only)	No. of measured traits in study, *d* (*h* only)	No. of populations, *d* (*h* only)
Artiodactyla	McDonald, 1981	*Bison antiquus–B. bison*	(2)	Fossil ts	171	74	3
Artiodactyla	Lister, 1989	*Cervus elaphus*	(2)	Fossil ts	10	10	2
Primates	Clyde and Gingerich, 1994	*Cantius torresi–C. trigonodus*	(2)	Fossil ts	22	2	12
Mammalia	Gingerich, 1994	*Haplomyous palust.–H. simpsoni*	(2)	Fossil ts	2	2	2
Mammalia	Gingerich, 1994	*Haplomyous si:sp*	(2)	Fossil ts	8	1	9
Foraminifera	Malmgren et al., 1983	*Globorotalia plesiotumida*	(2)	Fossil ts	8	1	9
Foraminifera	Malmgren et al., 1983	*G. plesiotumida*	(2)	Fossil ts	43	1	44
Foraminifera	Malmgren et al., 1983	*Globorotalia tumida*	(2)	Fossil ts	43	1	44
Foraminifera	Malmgren et al., 1983	*G. tumida*	(2)	Fossil ts	29	1	30
Foraminifera	Malmgren et al., 1983	*G. tumida*	(2)	Fossil ts	29	1	30
Foraminifera	Malmgren et al., 1983	*G. tumida*	(2)	Fossil ts	11	1	12
Foraminifera	Malmgren et al., 1983	*G. tumida*	(2)	Fossil ts	11	1	12
Foraminifera	Malmgren et al., 1983	*G. tumida*	(2)	Fossil ts	16	2	9
Artiodactyla	Klein, 1995	*Gazella sp.*	(2)	Fossil ts	7	1	8
Artiodactyla	Klein, 1995	*Gazella sp.*	(2)	Fossil ts	96 (26)	41	4
Proboscidea	Maglio, 1973	*Primeleph. gom.–Loxodonta afr.*	(2)	Fossil ts	50 (37)	20 (15)	5
Proboscidea	Maglio, 1973	*P. gom.–Elephas iolen.*	(2)	Fossil ts	31 (23)	15 (11)	4
Proboscidea	Maglio, 1973	*P. gom.–Elephas hysud.*	(2)	Fossil ts	71 (53)	24 (18)	5
Proboscidea	Maglio, 1973	*P. gom.–Mammuth. prim.*	(2)	Fossil ts	12	1	13
Artiodactyla	Prothero and Heaton, 1996	*Miniochoerus chad.–M. gracilis*	(2)	Fossil ts	57	1	58
Rodentia	Heaton, 1993	*Ischyromys parvidens–I. typus*	(2)	Fossil ts	70	1	71
Rodentia	Heaton, 1993	*I. parvidens–I. typus*	(2)	Fossil ts	42	2	22
Carnivora	Polly, 1998	*Viverravus acutus*	(2)	Fossil ts	158	1 (11)	1 (15)
Mollusca	Geary, 1990	*Peromyscus m. gracilis*	(2)	Fossil ts	9	1	10
Mollusca	Geary, 1990	*Melanopsis impressa*	(2)	Fossil ts	7	1	8
Mollusca	Geary, 1990	*Melanopsis fossilis*	(2)	Fossil ts	1	1	2
Perissodactyla	Haldane, 1949	*Melanopsis impressa: fossilis*	(2)	Fossil ts	6	2	4
Perissodactyla	Haldane, 1949	*Hyracotherium–Neohipparion*	(2)	Fossil ts	0 (3)	0 (1)	0 (4)
Dinosauria	Colbert, 1948	*Hyracotherium–Neohipparion*	(2)	Fossil ts	2	1	3
Dinosauria	Colbert, 1948	*Protoceratops–Triceratops*	(2)	Fossil ts	1	1	2
Dinosauria	Colbert, 1948	*Camptosaurus–Trachodon*	(2)	Fossil ts	1	1	2
Dinosauria	Colbert, 1948	*Polacanthus–Ankylosaurus*	(2)	Fossil ts	1	1	2
Dinosauria	Colbert, 1948	*Coelophysis–Tyrannosaurus*	(2)	Fossil ts	1	1	2
Dinosauria	Colbert, 1948	*Scelidosaurus–Stegosaurus*	(2)	Fossil ts	1	1	2
Hominidae	Ruff et al., 1997	*Homo*	(2)	Fossil ts	36	4	40
Rodentia	Barnosky, 1990	*Microtus pennsylvanicus*	(2)	Fossil ts	7	1	8
Rodentia	Barnosky, 1990	*M. pennsylvanicus*	(2)	Fossil ts	8	1	9
Rodentia	Barnosky, 1990	*M. pennsylvanicus*	(2)	Fossil ts	5	1	6
Radiolaria	Kellogg, 1975	*Pseudocubus verna*	This paper	Fossil ts	33	1	34
Carnivora	Kurten, 1959	*Ursus* sp.	This paper	Fossil ts	10	1	11

Table S2. Cont.

Taxa	Source	Species	Original database	Type of study	No. of divergence points, *d* (*h* only)	No. of measured traits in study, *d* (*h* only)	No. of populations, *d* (*h* only)
Carnivora	Kurten, 1959	*Felis silvestris* ssp.	This paper	Fossil ts	4	1	5
Carnivora	Kurten, 1959	*Felis lynx*	This paper	Fossil ts	1	1	2
Carnivora	Kurten, 1959	*Vulpes vulpes*	This paper	Fossil ts	2	1	3
Carnivora	Kurten, 1959	*Canis lupus*	This paper	Fossil ts	1	1	2
Carnivora	Kurten, 1959	*Putorius putorius*	This paper	Fossil ts	1	1	2
Carnivora	Kurten, 1959	*Martes martes*	This paper	Fossil ts	3	1	4
Carnivora	Kurten, 1959	*Gulo gulo*	This paper	Fossil ts	1	1	2
Carnivora	Kurten, 1959	*Meles meles*	This paper	Fossil ts	2	1	3
Carnivora	Kurten, 1959	*Lutra lutra*	This paper	Fossil ts	2	1	3
Rodentia	Kurten, 1959	*Apodemus sylvaticus*	This paper	Fossil ts	1	1	2
Total					5,087 (663)	645 (137)	1,631 (96)

Most data come from Hendry et al. (1) and Gingerich (2). A "field study" is defined as any study involving the collection of data on extant organisms. Synchronic studies are cross-sectional studies ("field-syn") whereas allochronic studies are longitudinal ("field-allo"). Number of divergence points is the total number of autonomous data points that were plotted for each type of divergence measure, with those data points for which *h* alone was measured in parentheses. Number of traits is the total number of different measurements that were used to obtain divergence (autonomous divergence only), and number of populations is the number of samples. Original databases indicate either Hendry et al. (1) or Gingerich (2). n.d., not determined.

*Dates for land-bridge islands are taken from Lu et al., 2002; Boback, 2003; Foufopoulos, 1999; Castilla, et al., 2008; Podner et al., 2004; Foufopolous and Ives, 1999; Villagran, 1988; and Case and Schwaner, 1993.

1. Hendry AP, Farrugia TJ, Kinnison MT (2008) Human influences on rates of phenotypic change in wild animal populations. *Mol Ecol* 17:20–29.
2. Gingerich PD (2001) Rates of evolution on the time scale of the evolutionary process. *Genetica* 112–113:127–144.

Table S3. Data sources for across-species comparative data

Taxa	Interval source	Divergence source	Original database	No. of taxa	No. of nodes	Trait
Squamates	Wiens et al., 2006	Wiens et al., 2006	This paper	259	258	SVL
Mammalia	Bininda-Emonds et al., 2007	Smith et al., 2004	This paper	3,264	1,770	(Mass)^1/3
Primates	Bininda-Emonds et al., 2007	Swindler, 2002	This paper	47	42	M/1 (MD)
Primates	Bininda-Emonds et al., 2007	Swindler, 2002	This paper	47	42	M/1 (TriB)
Aves	Sibley and Ahlquist, 1990	Dunning, 2008	This paper	121*	119	(Mass)^1/3
Aves	Thomas et al., 2004	Dunning, 2008	This paper	286	217	(Mass)^1/3
Aves	Filardi and Smith, 2005	Dunning, 2008	McPeek, 2008	12	11	(Mass)^1/3
Aves	Pérez-Emán, 2005	Dunning, 2008	McPeek, 2008	5	4	(Mass)^1/3
Aves	Eberhard and Bermingham, 2005	Dunning, 2008	McPeek, 2008	4	3	(Mass)^1/3
Aves	Eberhard and Bermingham, 2005	Dunning, 2008	McPeek, 2008	10	9	(Mass)^1/3
Aves	Lijtmaer et al., 2004	Dunning, 2008	McPeek, 2008	20	13	(Mass)^1/3
Aves	Austin, J. J., 1996	Dunning, 2008	McPeek, 2008	10	9	(Mass)^1/3
Aves	Chesser, R. T., 2000	Dunning, 2008	McPeek, 2008	7	6	(Mass)^1/3
Aves	Garcia-Moreno et al., 2001	Dunning, 2008	McPeek, 2008	20	17	(Mass)^1/3
Aves	Garcia-Moreno et al., 1999	Dunning, 2008	McPeek, 2008	9	8	(Mass)^1/3
Aves	Groombridge et al., 2004	Dunning, 2008	McPeek, 2008	7	6	(Mass)^1/3
Aves	Joseph et al., 2004	Dunning, 2008	McPeek, 2008	11	8	(Mass)^1/3
Aves	Klicka et al., 2003	Dunning, 2008	McPeek, 2008	6	5	(Mass)^1/3
Aves	Lee et al., 2003	Dunning, 2008	McPeek, 2008	3	2	(Mass)^1/3
Aves	Lucchini et al., 2001	Dunning, 2008	McPeek, 2008	12	11	(Mass)^1/3
Aves	Omland et al., 1999	Dunning, 2008	McPeek, 2008	22	18	(Mass)^1/3
Aves	Randi, 1996	Dunning, 2008	McPeek, 2008	5	4	(Mass)^1/3
Aves	Randi et al., 2001	Dunning, 2008	McPeek, 2008	5	4	(Mass)^1/3
Aves	Ribas and Miyaki, 2004	Dunning, 2008	McPeek, 2008	5	4	(Mass)^1/3
Aves	Weibel and Moore, 2002	Dunning, 2008	McPeek, 2008	19	18	(Mass)^1/3
Aves	Whittingham et al., 2002	Dunning, 2008	McPeek, 2008	8	7	(Mass)^1/3
Aves	Sorenson et al., 2004	Dunning, 2008	McPeek, 2008	18	11	(Mass)^1/3
Aves	Kimball et al., 2001	Dunning, 2008	McPeek, 2008	4	3	(Mass)^1/3
Aves	Cheviron et al., 2005	Dunning, 2008	McPeek, 2008	6	5	(Mass)^1/3
Aves	Gill et al., 2005	Dunning, 2008	McPeek, 2008	23	21	(Mass)^1/3
Aves	Given et al., 2005	Dunning, 2008	McPeek, 2008	9	7	(Mass)^1/3
Aves	Lovette and Bermingham, 1999	Dunning, 2008	McPeek, 2008	23	22	(Mass)^1/3
Aves	Mooers et al., 1999	Dunning, 2008	McPeek, 2008	11	10	(Mass)^1/3
Aves	Price et al., 2000	Dunning, 2008	McPeek, 2008	3	1	(Mass)^1/3
Aves	Ruolonen et al., 2000	Dunning, 2008	McPeek, 2008	7	6	(Mass)^1/3
Aves	Weckstein, 2005	Dunning, 2008	McPeek, 2008	6	5	(Mass)^1/3
Aves	Sato et al., 1999	Dunning, 2008	McPeek, 2008	12	10	(Mass)^1/3

*Taxa for this phylogeny are the family means rather than species-level means, with average values being calculated from Dunning (2008) for all taxa assigned to a given family. The phylogeny was scaled to a root age of 90 Myr.